Current Optics and Photonics
Vol. 2, No. 3, June 2018, pp. 241-249

ISSN: 2508-7266(Print) / ISSN: 2508-7274(Online)
DOI: https://doi.org/10.3807/COPP.2018.2.3.241

Infrared Dual-field-of-view Optical System Design with Electro-Optic/Laser Common-aperture Optics

Dohwan Jeong[1], Jun Ho Lee[1]*, Ho Jeong[2], Chang Min Ok[2], and Hyun-Woo Park[2]

[1]Department of Optical Engineering, Kongju National University, Cheonan 31080, Korea
[2]LIG Nex1 Co., Ltd., Yongin 16911, Korea

(Received April 6, 2018 : revised April 16, 2018 : accepted April 16, 2018)

We report a midinfrared dual-field-of-view (FOV) optical system design for an airborne electro-optical targeting system. To achieve miniaturization and weight reduction of the system, it has a common aperture and fore-optics for three different spectral wavelength bands: an electro-optic (EO) band (0.6~0.9 μm), a midinfrared (IR) band (3.6~4.9 μm), and a designation laser wavelength (1.064 μm). It is free to steer the line of sight by rotating the pitch and roll axes. Our design co-aligns the roll axis, and the line of sight therefore has a fixed entrance pupil position for all optical paths, unlike previously reported dual-FOV designs, which dispenses with image coregistration that is otherwise required. The fore-optics is essentially an achromatized, collimated beam reducer for all bands. Following the fore-optics, the bands are split into the dual-FOV IR path and the EO/laser path by a beam splitter. The subsequent dual-FOV IR path design consists of a zoom lens group and a relay lens group. The IR path with the fore-optics provides two stepwise FOVs (1.50° × 1.20° to 5.40° × 4.32°), due to the insertion of two Si lenses into the zoom lens group. The IR optical system is designed in such a way that the location and *f*-number (*f*/5.3) of the cold stop internally provided by the IR detector are maintained when changing the zoom. The design also satisfies several important performance requirements, including an on-axis modulation transfer function (MTF) that exceeds 10% at the Nyquist frequency of the IR detector pitch, with distortion of less than 2%.

Keywords : Common aperture, Dual-field-of-view, Lens design, Infrared optics, Optical system design
OCIS codes : (080.3620) Lens system design; (110.3080) Infrared imaging; (120.4570) Optical design of instruments

I. INTRODUCTION

In a modern electro-optical targeting system (EOTS), the importance of technologies for emitting laser light from an aircraft to a target on earth and recognizing and detecting the target has been emphasized, with the introduction of technologies capable of guiding a missile to a desired target. Existing electro-optical targeting systems have featured individual optical systems of independent structures, consisting of the electro-optics (EO) band, the infrared (IR) band, and a laser module [1-5]. The electro-optical targeting system has shown improved performance and functions according to the development of its operational methods, with developed optics that connects every module, and with a common structure of every optical system and optical window [6-9]. As a result, miniaturization and weight reduction have become possible, and the targeting accuracy of this system has improved due to the large-diameter optics. Figure 1 shows images of an individual aperture and a common-aperture EOTS.

The common-aperture EOTS shows enhanced tracking performance, due to the use of a dual field of view in the infrared optical system as in Fig. 2, to recognize a target accurately regardless of weather conditions and to meet users' requirements [10, 11]. The zoom lens system, which rapidly expands or shrinks the image of a target and has high accuracy, improves recognition and enhances tracking performance [12, 13]. Concerning the zoom lens system of

*Corresponding author: jhlsat@kongju.ac.kr, ORCID 0000-0002-4075-3504
Color versions of one or more of the figures in this paper are available online.

(a) Individual aperture EOTS (b) Common-aperture EOTS

FIG. 1. Images of (a) an individual and (b) a common-aperture EOTS.

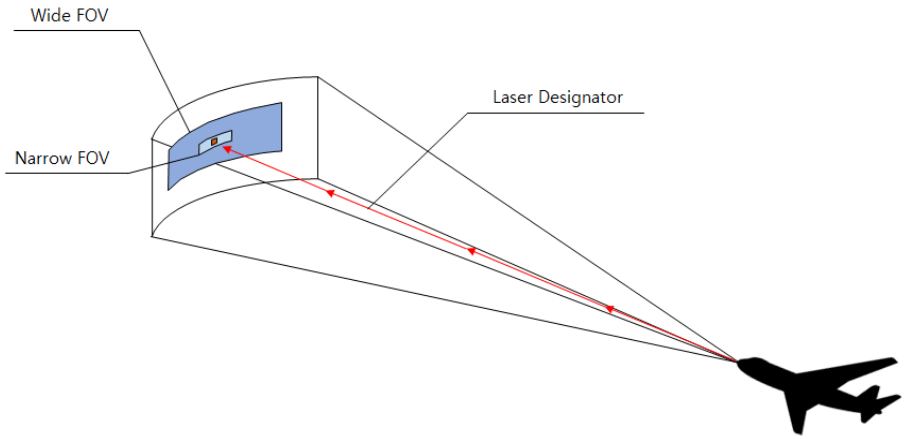

FIG. 2. Schematic diagram of a dual-field-of-view (FOV) targeting system with a laser designator [9].

the IR optical system, in a situation where the target should be recognized quickly and the response should be made immediately, the continuous zoom variation method has problems, in that speed becomes conspicuously slow, and chromatic aberrations and errors occur due to issues related to the optical axis alignment. Therefore, the stepwise zoom method of lens insertion is often utilized, to increase the optical axis stability and speed. The present optical system is designed with a common optical path and system that integrates the EO band, the IR band, and the laser module. Accordingly, it uses a common optical path shared by the laser module. As a result, the LOS (line of sight) error between the sensors at long distances is decreased considerably, thus improving the targeting accuracy as well.

We report here a midinfrared dual-field-of-view (FOV) optical system design for an airborne electro-optical targeting system. To achieve miniaturization and weight reduction of the system, it has a common aperture and fore-optics for three spectral wavelength bands (EO, IR, and the laser module). Housand *et al.* patented a compact optical design for a dual-FOV IR system with EO and laser common-aperture optics, as we here aim to achieve [14]. Figure 3 shows the schematic optical layout of the patented system. The optics is mechanically split into three groups (common aperture fore-optics, IR optics zoom and relay group, and IR focus and laser group) to provide pitch and roll axis rotation of the light of sight. The entire optics, apart from the third group, can rotate around the front-to-back axis (roll), and the common-aperture fore-optics can rotate around the side-to-side axis (pitch). However, this design has an axis offset between the line of sight and the roll axis, which causes a nonuniform pupil shift as the system rolls around.

We modified the earlier design to have a fixed pupil position by co-aligning the line of sight and the roll axis. The fore-optics in the roll group is essentially an achromatized, collimated beam reducer for all bands. Following the fore-optics, the bands are split into the IR path and the EO/laser path by a beam splitter. The IR path then consists of a zoom lens group and a relay lens group. The IR path with the fore-optics provides two stepwise narrow and wide FOVs (1.50° × 1.20° to 5.40° × 4.32°), due to the insertion of another lens group into the zoom lens group. The following sections first describe the system approach, and then report the dual-FOV IR paths in detail, with analyzed performances.

II. SYSTEM DESIGN

2.1. System Requirements

We report a midinfrared dual-field-of-view (FOV) optical system design for an airborne electro-optical targeting system. To achieve miniaturization and weight reduction of the system, it has a common aperture and fore-optics for three spectral wavelength bands: an electro-optic (EO) band (0.6~0.9 μm), a midinfrared (IR) band (3.6~4.9 μm), and a designation laser wavelength (1.064 μm). Figure 3 shows the optical layout of the common-aperture targeting system that we report herein. It has a common optical axis for roll-axis rotation and the line of sight (LOS), and therefore does not have the entrance pupil shift reported in previous work while it rolls the fore-optics group.

The IR imaging system serves to record an IR image of a target at a distance from an IR detector with a resolution of 1280 × 1024 square pixels and a pixel pitch of 15 μm, in the thermal IR spectrum from 3.6 to 4.9 μm. The IR optics should provide two stepwise fields of view (narrow and wide). The wide field of view (WFOV, 5.4° × 4.3°) is 3.6 times as large as the narrow field of view (NFOV, 1.5° × 1.2°). We use the wide-FOV image first to find the target, and then the narrow-FOV image to recognize it. The dual-IR optics design should have the same stop position and *f*-number (*f*/5.3) conjugated to the cold stop internally provided by the IR detector. Table 1 tabulates the design requirements of the dual-FOV IR optical system.

2.2. Layout Design

To reduce the size of the overall optical system, we apply common-aperture fore-optics for the EO band, the IR band, and the laser designation. The IR optical system and the laser module share a common optical path, and are designed such that a beam of light is split into the two paths using a beam splitter. Figure 4 shows a schematic layout of the design, while Fig. 5 shows the three-dimensional layout of the design. Here we report the IR path in detail.

The IR path design consists of fore-optics, the zoom lens and relay lens, followed by the IR detector in sequence. Fold mirrors and beam splitters are also used to provide a compact layout, as well as roll and pitch axis rotation of the line of sight. The roll axis is co-aligned to the line of sight so that the entrance pupil position is kept constant

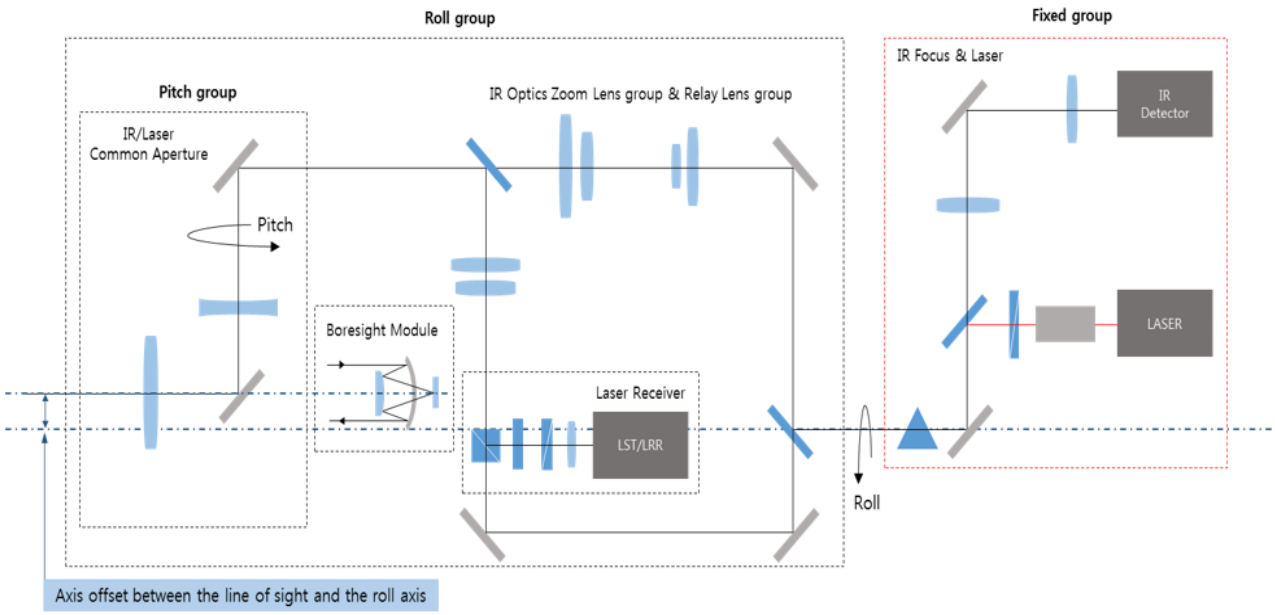

FIG. 3. Schematic optical layout of a previously reported EO/IR common-aperture system [14].

TABLE 1. Design requirements of the dual-FOV IR optical system

Operating wavelength range	3.6~4.9 μm
Field of view (FOV)	1.5° × 1.2° (NFOV), 5.4° × 4.3° (WFOV)
f-number	*f*/5.3
Sensor pixel size	15 μm × 15 μm
Sensor array format	1280 × 1024
MTF	≥ 10% @ 33 lp/mm, on axis
Distortion	≤ 2%

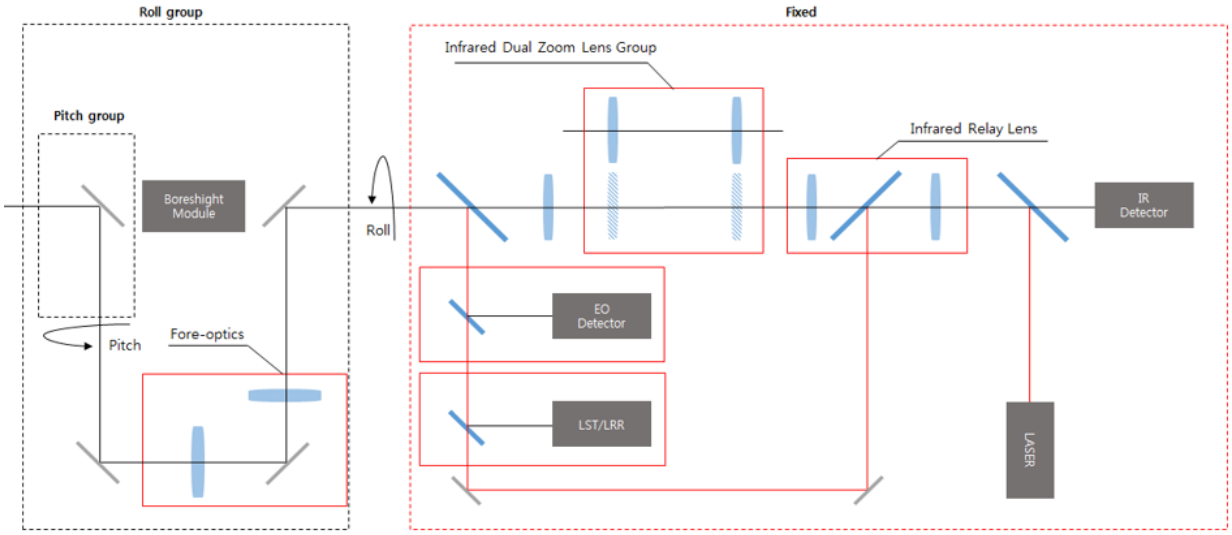

FIG. 4. Schematic optical layout of the common-aperture targeting system that we report herein.

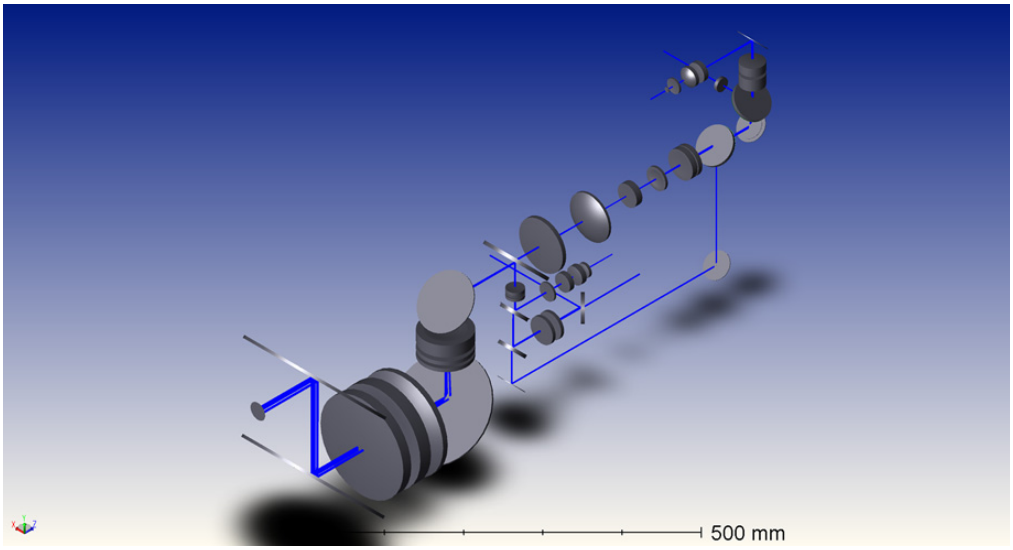

FIG. 5. Three-dimensional optical layout of the design.

as the optics rolls around, which eliminates the image coregistration process that would be required otherwise. The fore-optics is essentially an achromatized, collimated beam reducer for all bands. Following the fore-optics, the bands are split into the dual-FOV IR path and the EO/laser path by a beam splitter. The following dual-FOV IR path design consists of a zoom lens group and a relay lens group.

III. DUAL-FOV IR OPTICS DESIGN

3.1. Fore-optics

The fore-optics should be composed of materials with good transmittance over the wide spectrum from 0.6~4.9 μm, as it is common for all three bands: EO (0.7~0.9 μm), IR (3.6~4.9 μm) and the designation laser (1.064 μm) [14]. Table 2 lists six optical materials (BaF_2, CaF_2, Spinel, MgF_2, ZnS, and ZnSe) having relatively high transmittance over a wide spectrum. However, after an investigation of the availability, birefringence, and manufacturing ease of these materials, only three materials (BaF_2, MgF_2, and ZnS) were ultimately chosen for the fore-optics design [15-17]. Table 2 lists the optical properties of the selected materials.

The fore-optics is essentially a collimated beam reducer with a 3.75 reduction ratio, achromatized for all bands, consisting of the two lens groups. Figure 6 shows each beam path for the four bands. The stop position and size of each path are predetermined in the system layout design. Specifically, the stops of the IR paths are conjugated to the cold stop of the IR detector by the subsequent IR paths. Each group is initially designed with a combination

TABLE 2. Optical properties of the selected materials for 0.7~4.9 μm [15]

Properties	Index of refraction (n)			Abbe numbers (V)			Partial dispersion (P)		
Wavelength (μm)	0.6~0.9	1.0~1.6	3.3~5.0	0.6~0.9	1.0~1.6	3.3~5.0	0.6~0.9	1.0~1.6	3.3~5.0
BaF_2	1.47	1.46	1.45	191.4	229.4	50.8	0.59	0.56	0.45
CaF_2	1.43	1.42	1.40	201.8	167.5	24.5	0.57	0.52	0.44
Spinel	1.70	1.70	1.68	123.7	91.9	10.2	0.56	0.51	0.43
MgF_2	1.37	1.37	1.34	205.4	132.7	15.1	0.56	0.5	0.44
ZnS	2.31	2.27	2.25	42.5	73.5	133.0	0.6	0.63	0.48
ZnSe	2.52	2.46	2.43	28.5	53.6	218.4	0.61	0.64	0.53

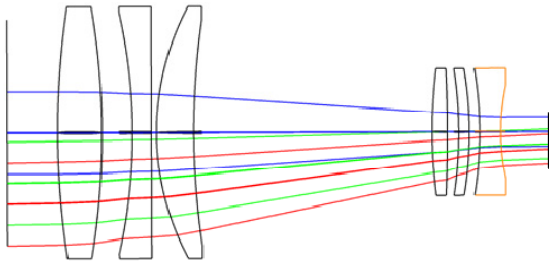

(a) EO path (0.6~0.9 μm)

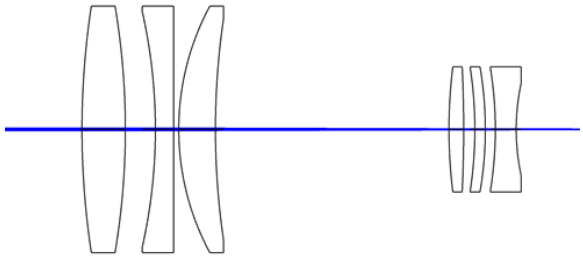

(b) Designator laser path (1.064 μm)

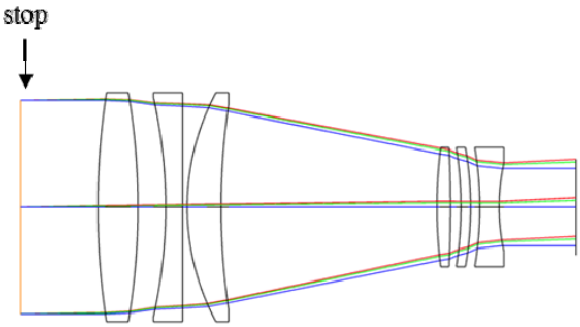

(c) IR NFOV path (3.3~5.0 μm)

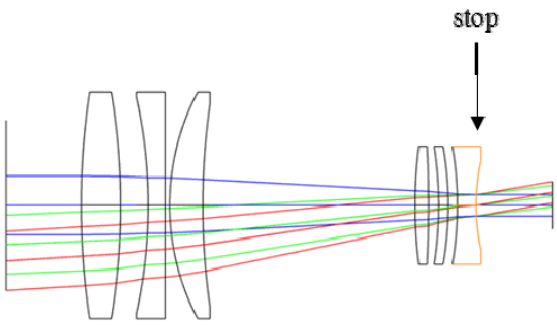

(d) IR WFOV path (3.3~5.0 μm)

FIG. 6. Fore-optics beam paths for the four different wavebands (EO, designator laser, IR NFOV, and IR WFOV).

of three types of glass (BaF_2, MgF_2, and ZnS), to remove partial dispersion and minor residual chromatic aberrations, using Eqs. (1)~(3). During the selection of the combination of the material, we attempt to minimize the root-mean-square (RMS) of each optical power, as represented by W in Eq. (4), to minimize spherical aberration. This parameter has the advantage of being independent of the lens magnification, aperture size, and angle of view parameters. The two optics groups are then combined and re-optimized together.

$$K_1 + K_2 + K_3 = K, \tag{1}$$

$$\frac{K_1}{V_1} + \frac{K_2}{V_2} + \frac{K_3}{V_3} = 0, \tag{2}$$

$$\frac{K_1}{V_1} P_1 + \frac{K_2}{V_2} P_2 + \frac{K_3}{V_3} P_3 = 0, \tag{3}$$

$$W = \left(\frac{1}{N} \sum K_i^2 \right)^{1/2} = \left[\frac{1}{3} (K_1^2 + K_2^2 + K_3^2) \right]^{1/2}, \tag{4}$$

3.2. Dual-FOV Stepwise Zoom Design

The following IR path is then designed using germanium and silicon, both of which have satisfactory transmittance in the IR band. Zoom-lens compensation methods include mechanical, optical, and electronic compensation systems. Among them, this paper uses a mechanical compensation system, consisting of a zoom lens group for magnification conversion and a compensation lens group for correction of the image plane and position variation [18]. The mechanical compensation system includes a continuous zoom optics system, in which the arrangement of the lenses changes continuously, and a stepwise zoom optics system, in which the magnification ratio is changed by inserting another lens group. Figure 7 below shows the stepwise zoom optical system that flips the lens in and out.

3.3. Relay Lens Design

In the IR optical system configuration, the relay lens group is located behind the IR zoom lens group. The relay lens group is designed to conjugate the image formed by the fore-optics and the IR zoom lens group to an intermediate image to the IR cold stop conjugation optics, as reported in the next section. Figure 8 shows a schematic diagram of the relay optics, and Fig. 9 shows the two optical layouts for the NFOV and WFOV IR paths.

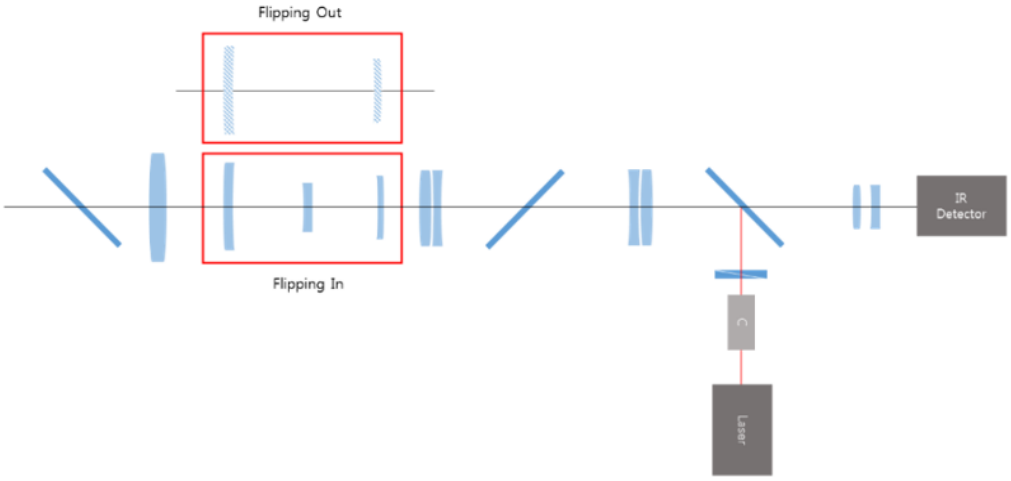

FIG. 7. The flipping in/out dual-FOV zoom optical system layout.

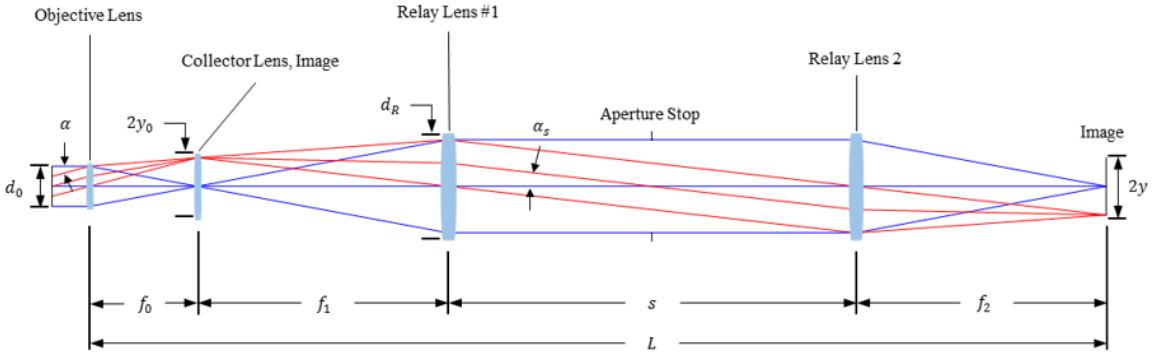

FIG. 8. Conceptual relay lens configuration.

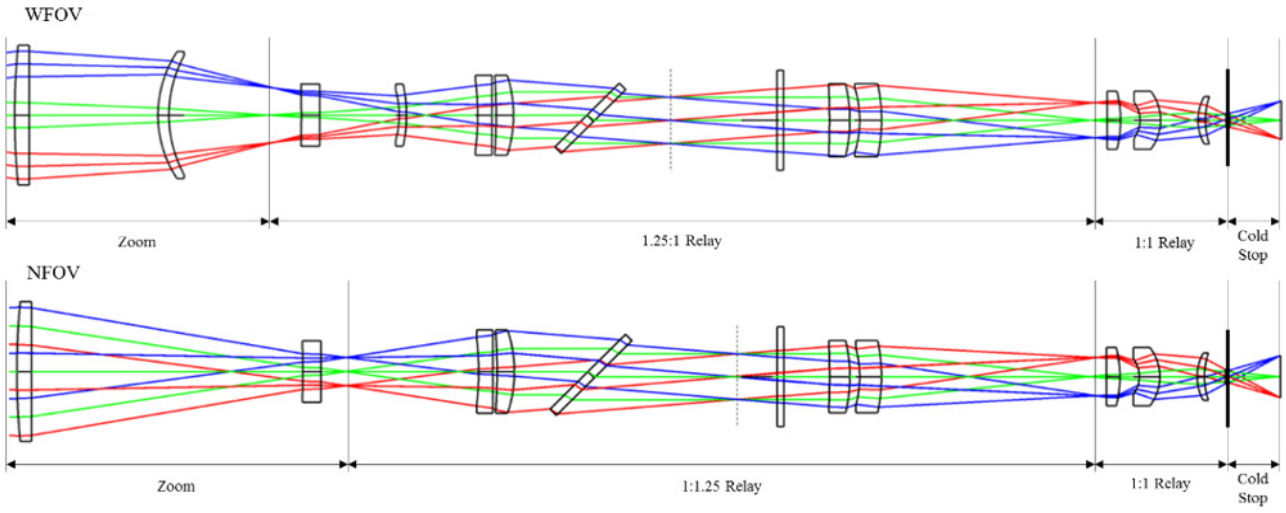

FIG. 9. Two optical relay and cold stop conjugation layouts, for the NFOV and WFOV IR paths respectively.

3.4. Cold Stop Conjugation

The IR optical system uses a detector sensitive to thermal radiation, and cools to the liquid-nitrogen temperature range for increased sensitivity. The detector has a cold shield to increase the sensitivity, and plays a role in limiting the amount of warm background flux. Cameras operating in the thermal infrared band (mid- and long-wavelength IR) use a cold stop designed to match the exit pupil of the optics, to avoid parasitic radiation or vignetting, using 100% of the cold stop efficiency [19].

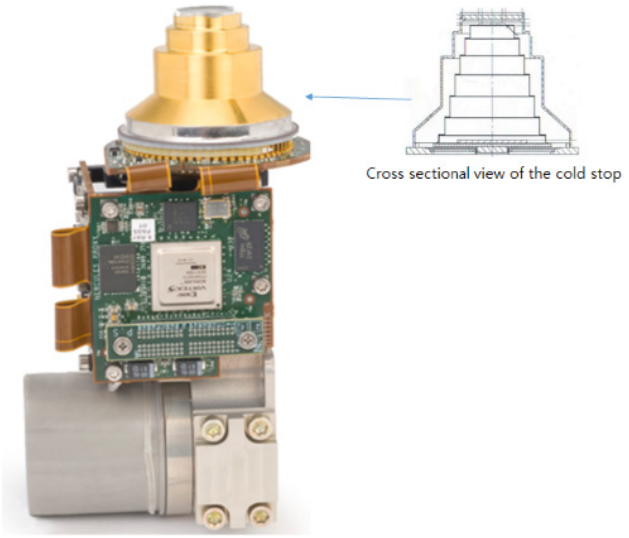

FIG. 10. Image of the IR detector, with a cross-sectional view of the cold stop.

An *f*-number-matched optical system and an IR camera are required to ensure optimal image quality in the thermal IR. The IR optical system is designed in such a way that the location and *f*-number (*f*/5.3) of the cold stop internally provided by the IR detector are maintained when changing the zoom. Figure 10 shows an image of the IR detector and the corresponding cross-sectional view of the cold stop; the cold stop conjugation is also shown in Fig. 11.

3.5. Overall Design

The overall lens layouts for the narrow- and wide-FOV IR paths are plotted in Fig. 11. Figure 12 plots an equivalent folded optical layout of the narrow-field-of-view IR path. Figures 13 and 14 show the optical performances of the NFOV and WFOV IR path designs respectively. At the Nyquist frequency of the detector, *i.e.* 33 lp/mm, the on-axis MTFs of both designs exceed 14%. The distortion of the entire narrow-field optical system is less than 2% and 1% on the NFOV and the WFOV paths respectively.

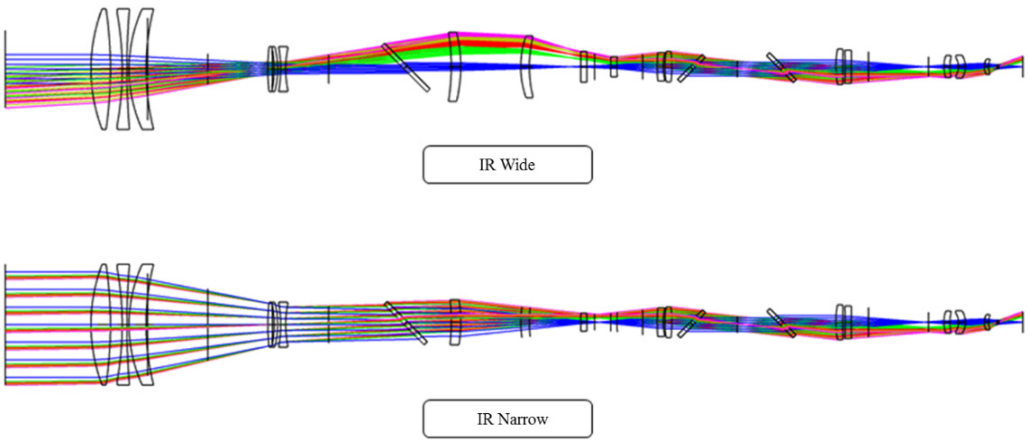

FIG. 11. Unfolded overall optical layout of the narrow- and wide-FOV IR paths.

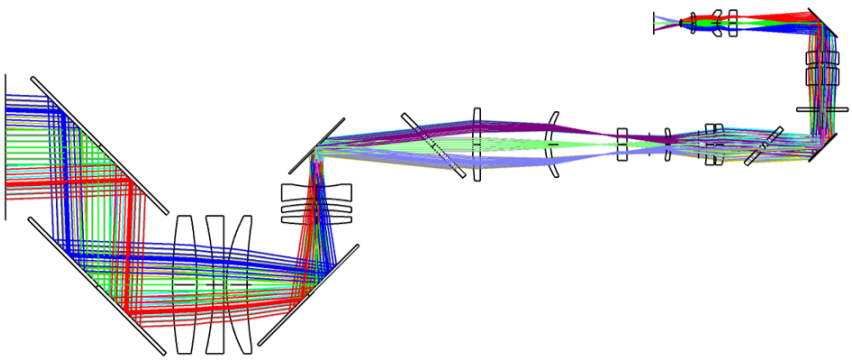

FIG. 12. Folded optical layout of the wide-FOV IR path.

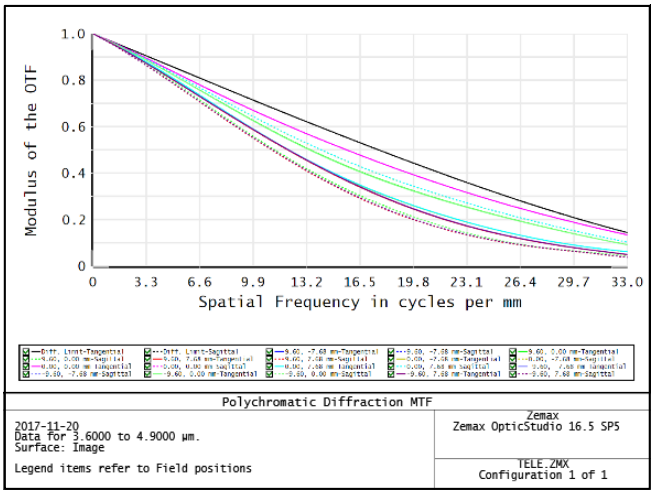

(a) MTF

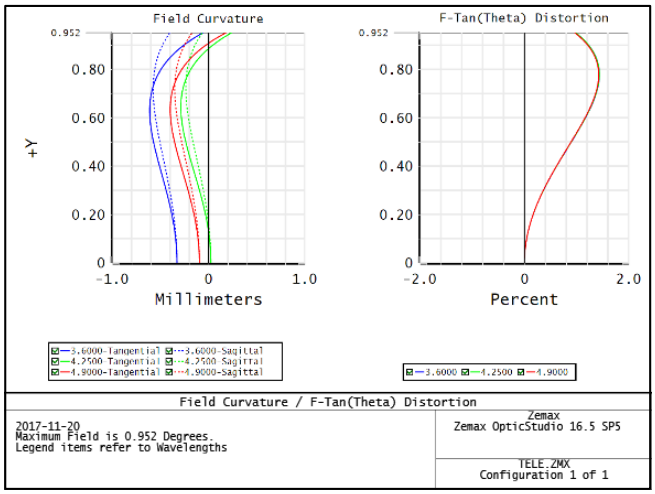

(b) Field curvature and distortion plot

FIG. 13. Narrow-field-of-view IR optical system performance.

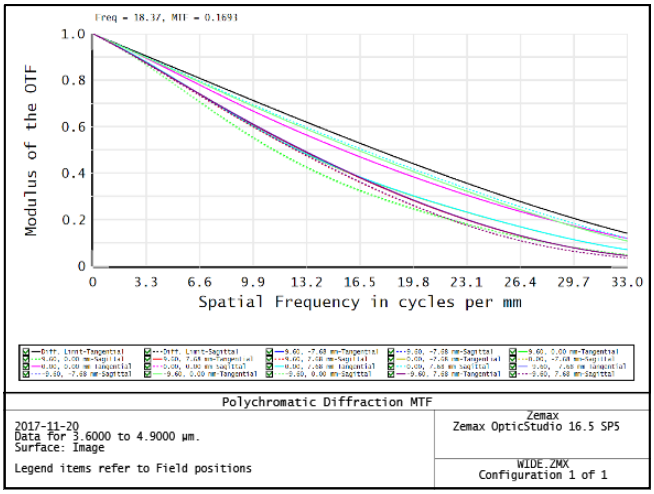

(a) MTF

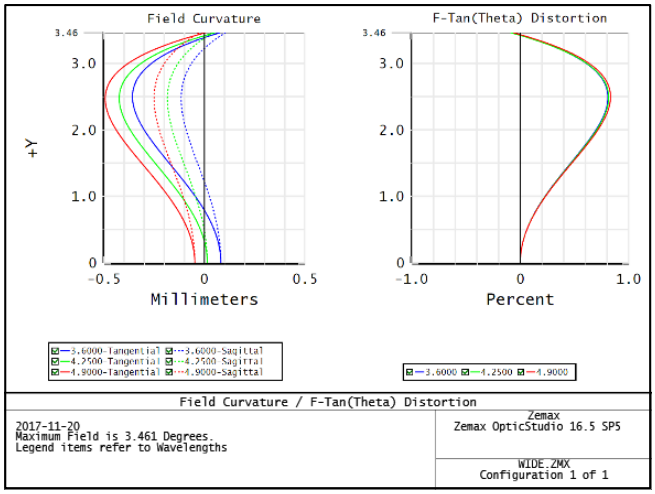

(b) Field curvature and distortion plot

FIG. 14. Wide-field-of-view IR optical system performance.

IV. CONCLUSION

This paper proposes a dual-FOV IR optical system with a common aperture for the EO band (0.7~0.9 µm), the IR band (3.6~4.9 µm), and the designator laser (1.064 µm). It provides roll and pitch axis rotation to steer the line of sight. Our design is initially proposed to co-align the roll axis, and the line of sight consequently has a fixed entrance pupil position for all optical paths.

The proposed design following the IR path consists of a common aperture and fore-optics, an IR zoom lens group, an IR relay lens group, and IR stop conjugation optics. The fore-optics is essentially an achromatized, collimated beam reducer for four different wavebands (EO, designator laser, IR NFOV, and IR WFOV). Following the fore-optics, the bands are split into a dual-FOV IR path and an EO/laser path by a beam splitter. The subsequent dual-FOV IR path design consists of a zoom lens group and a relay lens group. The IR path with the fore-optics provides two stepwise FOVs (1.50° × 1.20° to 5.40° × 4.32°), due to the insertion of two Si lenses into the zoom lens group. The IR optical system is designed in such a way that the location and *f*-number (*f*/5.3) of the cold stop internally provided by the IR detector are maintained when changing the zoom.

The reported design satisfies several notable performance requirements, including on-axis MTF > 10% at the Nyquist frequency of the IR detector pitch, and distortion below 2%. Further research can concentrate on thermal stability during optical performance of the design.

ACKNOWLEDGMENT

This work was supported by LIG Nex1.

REFERENCES

1. H. Vogel and H. Schlemmer, "Dual-band infrared camera," Proc. SPIE **5964**, 59640S-2 (2005).
2. I. Clark, "Exploitation of EO Technologies from the EMRS DTC," Proc. SPIE **6739**, 67390K (2007).
3. Y. Yoon, G. Yu, C. Noh, and D. Song, "Robust scanning scheme over large area for airborne EO/IR camera," Proc. SPIE **8185**, 81850X-1 (2011).
4. L. Zhang, J. Lai, and Y. Huang, "Design of visible/long-wave infrared dual-band imaging optical system," Proc. SPIE **10154**, 101540V-1 (2016).
5. M. Gerken, J. Fritze, M. Munzberg, and M. Weispfenning, "Military reconnaissance platform for the spectral range from the visible to the MWIR," Proc. SPIE **10177**, 101770C-1 (2017).
6. J. Lee, Y. Jung, S. Ryoo, Y. Kim, B. Park, H. Kim, S. Youn, K. Park, and H. Lee, "Imaging performance analysis of an EO/IR dual band airborne camera," J. Opt. Soc. Korea **15**, 174-181 (2011).
7. S. Seong, J. Yua, D. Ryu, J. Hong, J. Yoon, S. Kim, J. Lee, and M. Shin, "Imaging and radiometric performance simulation for a new high performance dual band airborne reconnaissance camera," Proc. SPIE **7307**, 730705 (2009).
8. A. Mahmoud, D. Xu, and L. Xu, "Optical design of high resolution and shared aperture electro-optical/infrared sensor for UAV remote sensing applications," in *Proc. IEEE International Geoscience and Remote Sensing Symposium* (China, Nov. 2016), pp. 2921-2924.
9. W.-J. Chang, X.-Z. Zhang, Y.-D. Luan, and B. Zhang, "Dual FOV infrared lens design with the laser common aperture optics," Proc. SPIE **9449**, 94492B (2015).
10. R. G. Sementelli, "EO/IR dual-band reconnaissance system DB-110," Proc. SPIE **2555**, 222-231 (1995).
11. Y. Nevo, "Dual-band optics," Opt. Eng. **52**, 053002 (2013).
12. S. Pal and L. Hazra, "Structure design of mechanically compensated zoom lenses by evolutionary programming," Opt. Eng. **51**, 063001 (2012).
13. K.-L. Huang, "Synthesis of first order designs of optically compensated catadioptric zoom optical systems," Proc. SPIE **3129**, 108-118 (1997).
14. B. J. Housand and S. J. Jesse, "Combined laser/FLIR optics system," US Patent No. 6,359,681 B1 (2002).
15. P. Klocek, *Handbook of Infrared Optical Materials* (Marcel Dekker Inc., New York, USA, 1991).
16. G. E. Wiese and F. Dumont, "Refractive multispectral objective lens system and methods of selecting optical materials therefor," US Patent No. 6,950,243 B2 (2005).
17. D. Ren and J. R. Allington-Smith, "Apochromatic lenses for near-infrared astronomical instruments," Opt. Eng. **38**, 537-542 (1999).
18. A. Miks and J. Novak, "Paraxial analysis of three-component zoom lens with fixed distance between object and image points and fixed position of image-space focal point," Opt. Express **22**, 15571-15576 (2014).
19. N. Gat, J. Zhang, M. D. Li, L. Chen, and H. Gurrola, "Variable cold stop for matching IR cameras to multiple *f*-number optics," Proc. SPIE **6542**, 65420Y (2007).